

## PETROPHYSICAL AND RESERVOIR CHARACTERISTICS OF SEDIMENTARY ROCKS FROM OFFSHORE WEST BARAM DELTA, SARAWAK BASIN, MALAYSIA

Joel Ben-Awuah<sup>1,2</sup>, Eswaran Padmanabhan<sup>2</sup>, Spariharijaona Andriamihaja<sup>2</sup>, Prince Ofori Amponsah<sup>3</sup> and Yasir Ibrahim<sup>2</sup>

<sup>1</sup> Department of Petroleum Engineering, Faculty of Engineering, Technology and Built Environment, UCSI University, Jalan Choo Lip Kung, Taman Taynton View, 5600 Cheras, Kuala Lumpur, Malaysia

<sup>2</sup> Department of Geosciences, Faculty of Geosciences and Petroleum Engineering, Universiti Teknologi PETRONAS, Bander Seri Iskandar, 31750 Tronoh, Perak Darul Ridzuan, Malaysia

<sup>3</sup> Azumah Resources Limited, Private Mail Bag CT 452, Cantonments, Accra, Ghana

Received May 26, 2016; Accepted July 1, 2016

---

### Abstract

Sedimentary successions in the Baram Delta consist mainly of alternating sandstones and siltstones with rare intercalations of mudstones. This study examines the petrophysical variations between these Middle to Upper Miocene sedimentary facies with emphasis on porosity, permeability, pore size distribution, displacement pressure and irreducible water saturation. Over 130 core samples retrieved from seven offshore wells in four fields of the West Baram Delta were analyzed using thin sections, SEM with EDX, poroperm and mercury porosimetry. Six sandstone facies were identified in the studied wells including coarse grained sandstones, very fine grained sandstones, fine grained massive sandstones, bioturbated sandstones and parallel laminated sandstones. Average porosity and permeability respectively for the sandstone facies are 24.97% and 1910.6mD for coarse grained sandstones, 5.66% and 1.4mD for very fine grained sandstones, 16.48% and 23.28mD for bioturbated sandstone, 19.75% and 113.17mD for parallel laminated sandstones, 19.85% and 100.36mD for poorly sorted fine grained massive sandstone and 24.65% and 402.14mD for moderately sorted fine grained massive sandstones. The results indicate that the coarse grained sandstones are the best in terms of reservoir rock quality compared to the very fine grained sandstones that have the worst reservoir rock characteristics. The excellent reservoir rock quality in the coarse sandstones is attributed to its lack of cement between grains, very good intergranular porosity and pore connectivity. The poor reservoir rock quality in the very fine sandstone is attributed to its high degree of consolidation, lack of pores and high amount of cement and matrix between grains. A significant reduction in porosity and permeability is observed in the bioturbated sandstones due to the concentration of clays, heavy minerals and pyrite within burrows by burrowing organisms resulting in localized reduction in porosity.

**Keywords:** West Baram Delta; Sarawak Basin; Porosity; Permeability; Reservoir properties.

---

### 1. Introduction

An integral part of reservoir characterization usually involves a detailed evaluation of rock facies and their corresponding characteristics. However, the evaluation of such sedimentary rock facies are often complicated by complexities in depositional environment, composition, texture, structure and petrophysical properties. These rock facies are masses of rocks which can be defined and distinguished from others by its geometry, lithology, sedimentary structures, palaeocurrent pattern and fossils [1]. These defining parameters often induce different forms of heterogeneities in facies distribution and facies characteristics. Such heterogeneities in facies characteristics refer to vertical and lateral variations in facies such as texture, structure, porosity, permeability, and/or capillarity [2-4]. Reservoir heterogeneity in sandstone bodies occur at various extents and scales, ranging from micrometers to hundreds of meters, and is

commonly attributed to variations in depositional facies, diagenesis, and structural features such as the presence of fractures and faults [5]. Heterogeneity in facies distribution and facies characteristics of a petroleum reservoir is a vital factor when identifying exploration targets, the performance of an enhanced recovery project, well placements, field development plans and displacement mechanisms [6-7].

The study area of this research is the prolific Baram Delta province, offshore Sarawak (Fig.1). Several studies on sedimentology [8-16] and tectonic evolution [17-20] of the Baram delta have been carried out over the years. Such studies have typically focused on basin formation, deposition and distribution of facies in the delta. However, very little studies is available on petrophysical characteristics of identified facies in the delta. The objective of this paper therefore is to investigate variations in selected petrophysical and reservoir properties of sedimentary facies in four fields of the Baram Delta.

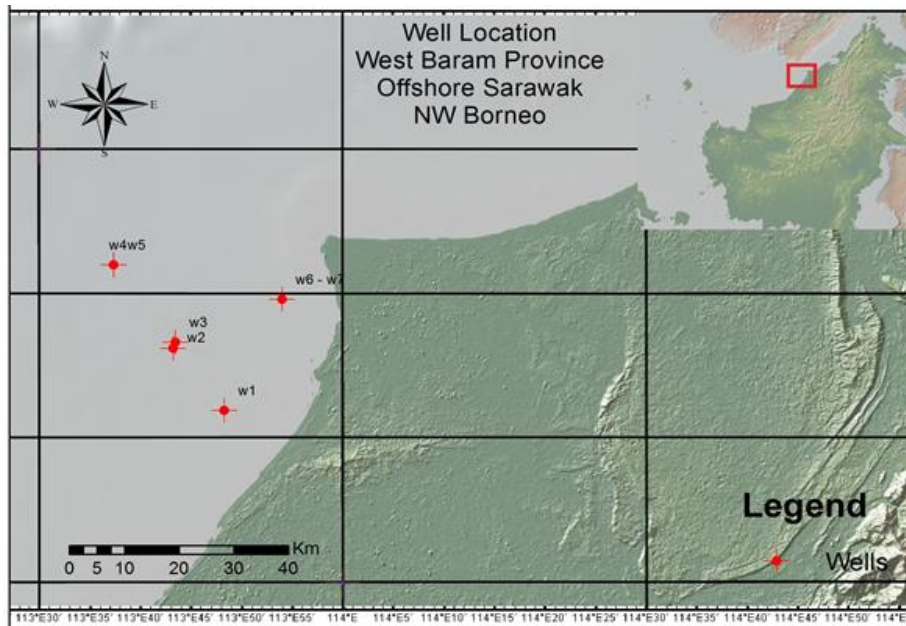


Fig.1. Location map of the Baram Delta province, offshore Sarawak (modified after [19])

## 2. Geologic setting

The Baram Delta is one of seven geological provinces found offshore the Sarawak foreland Basin [17-18] and is the most prolific of all the geological provinces in the basin [10] (Fig.1). The delta which was discovered in 1969 is estimated to have more than 400 million stock barrels of oil in place with multiple stacked sandstone reservoirs in a shallow offshore environment and has been in production for the past 30 years [21]. The Baram Delta consists of nine fields with an average recovery factor of about 30% [22]. The Baram Delta was formed on an active continental margin with its shape and size suggesting that it may have developed initially as a pull apart basin whose length and width were pre-determined by its bounding faults [10]. It extends from the northern part of Sarawak to the southern part of Sabah. The part of the delta in the Sarawak basin is known as the West Baram Delta and spans an area of 7500square km with 2500square km of it onshore [8, 23]. A major northeast-hading fault zone known as the West Baram Line forms the Western margin of the province and separates the delta from the older and more stable Balingian and Central Luconia Province [16].

The stratigraphic architecture of the delta was constructed by Middle to Upper Miocene thick and sandy progradational shallow marine-deltaic sequences which are separated by transgressive marine shale intervals [10]. Eight sedimentary cycles which were identified by [8] in nearby provinces in the Sarawak Basin were also extended to the Baram Delta by [24]. Johnson *et al.* proposed that these cycles are clastic or carbonate successions separated by

prominent shale intervals deposited during rapid transgression. The Baram Delta reservoir rocks belong to cycles IV to VII [10].

### 3. Materials and methods

The study involves 7 wells from 4 fields in the West Baram Delta. The cored intervals studied are Middle to Upper Miocene in age and are mainly Cycles V and VI deposits. Facies identification and distribution studies were carried out by core logging with emphasis on texture (grain size, grain sorting and grain shape), structure and bioturbation. The facies characterization was supported with petrographic studies that includes thin section studies and scanning electron microscope (SEM) with energy dispersive X-ray (EDX). Petrophysical studies was done using mercury porosimetry and unsteady gas permeameter and porosimeter.

The objective of the thin sections study was for microscopic examination of the rocks. The microscopic examination of sediments is an essential tool in the description and interpretation of sediments [25]. The thin sections were made according to procedures described by [26-27]. The samples were impregnated with a blue epoxy for easy identification of porosity. A petrographic microscope was used in describing the thin sections.

Samples of 2cm x 2cm dimension of each core slab were taken for scanning electron microscopy (SEM). High magnification photomicrographs of samples were taken for enhanced description of textures, pores, pore fillings, microstructures and inferences on diagenetic and depositional processes according to [28-29]. The SEM analysis was done using a Carl Zeiss Supra 55 variable pressure field emission scanning electron microscope (VP FESEM) with variable pressure ranging from 2Pa to 133Pa and probe current between 1pA to 10nA. Magnifications of x 100 up to x 10000 were used. Energy dispersive X-ray spectroscopy (EDX) was carried out to generate elemental distribution maps of the samples using an Oxford Instruments EDX detector.

A Thermo Scientific PASCAL 240 Series Mercury Porosimeter was used for the measurement in this study. Samples were cleaned with a Cole-Parmer Ultrasonic Cleaner, weighed in both water and air and the measurement taken by injection of mercury into the sample at high pressure. A maximum test pressure of 200MPa, at a temperature of 25°C and mercury density of 13.534g/cm<sup>3</sup> were used. The equipment is programmed to automatically correct for variations in compressibility of samples. Parameters of interest for this study were pore diameter, pore size distribution, total pore volume, total pore surface area and porosity.

Porosity and permeability were measured in 131 samples to assess reservoir quality in the rocks. Core plug permeability was measured at ambient confining pressure using a Vinci Technologies unsteady gas permeameter and porosimeter, Coreval 30 Poro-perm equipment. The core plugs used had a 1 inch diameter and 3 inches length. The Coreval 30 equipment is both a permeameter and porosimeter and so measures both permeability and porosity. It uses helium gas to measure porosity and permeability of samples. The unsteady state pressure drop method is used to measure gas permeability and the liquid permeability (Klinkenberg corrected permeability) are calculated. The equipment can measure permeability within the range of 0.001md-10D and porosity of up to 60%. The method used in this research is the American Petroleum Institute recommendation practice 40 (API RP 40). A maximum confining pressure of 400Psi, room temperature ranging between 25-27°C and humidity range of 65-71% were used.

## 4. RESULTS AND DISCUSSION

### 4.1. Petrography

#### 4.1.1. Coarse grained sandstone

The coarse grained sandstones are composed mainly by quartz grains with minor amount of clays, feldspars and iron oxides (Figs.2a and 2d). They have subrounded and moderately sorted grains with predominantly coarse grains ranging in size between 387-980microns (Figs.2a and 2b). There is an apparent lack of matrix and cement between grains resulting in high porosity and very good pore connectivity. They have an average porosity of 25% and

permeability of 1910.6mD (Table 1). The pore type is mainly intergranular porosity with minor intragranular porosity from mineral alteration.

Table 1. Porosity and permeability statistics of the different facies

Facies	Statistics	Porosity (%)	Permeability (mD)
Coarse grained sandstones (n=12)	Min	21.5	1250.2
	Max	30.42	2913.56
	Mean	24.97	1910.60
	St. dev.	2.41	674.55
Bioturbated sandstones (n=23)	Min	10.6	5.95
	Max	19.7	47.9
	Mean	16.48	23.28
	St. dev.	2.62	15.1
Moderately sorted fine sandstone (n=41)	Min	17.7	223.33
	Max	32.1	672.84
	Mean	24.65	402.14
	St. dev.	3.15	142.78
Poorly sorted fine sandstones (n=17)	Min	16.7	52.27
	Max	23.4	172
	Mean	19.85	100.36
	St. dev.	2.15	37.12
Laminated sandstones (n=15)	Min	15.35	64.31
	Max	23.1	163.53
	Mean	19.75	113.17
	St. dev.	2.28	33.62
Very fine grained sandstones (n=23)	Min	0.17	0.1
	Max	13.5	5.39
	Mean	5.66	1.4
	St. dev.	4.51	1.58

#### 4.1.2. Very fine grained sandstone

The very fine grained sandstones are composed mainly by quartz grains and siderite cement (Fig.3a). They are heavily cemented with very high matrix content and very low porosity (Figs.3a, 3b and 3c). Most of the pores have been filled by cement. They have an average porosity of 5.7% and permeability of 1.4mD (Table 1). The matrix is made up of very fine quartz, iron oxides and siderite (Figs.3a and 3d). They have angular and poorly sorted grains with predominantly very fine grains ranging in size between 75-245microns (Fig.3a).

#### 4.1.3. Bioturbated sandstones

The bioturbated sandstones are composed mainly by quartz grains, feldspars, clays and iron oxides (Figs.4a-4f). SEM images show that the clays are mainly kaolinite (Fig.4d).

There is non-uniform distribution of matrix between the sandstone matrix and burrows (Fig.4a). The burrows have high matrix density with the burrow fill composed of a mixture of pyrite, iron oxides, kaolinite, silt sized quartz and heavy minerals such as titanium and manganese (Fig. 4c) [30-32]. There is therefore a marked difference in porosity and pore connectivity between the burrows and sandstone matrix. The burrows have lower porosity compared to the sandstone matrix which have higher porosity and better pore connectivity. These sandstones have an average porosity of 16.7% and permeability of 23.4mD (Table 1). The bioturbated sandstones therefore have lower porosity than the non-bioturbated sandstones. They have subangular and poorly sorted grains with predominantly fine grains and show a burrow mottling texture.

#### **4.1.4. Laminated sandstone**

The laminated sandstones are composed mainly by quartz grains, clays (kaolinite), feldspars and iron oxides (Figs.5a-5d). They have subangular and poorly sorted grains with predominantly fine grains ranging in size between 35-186microns (Figs.5a and 5b). The laminations consist of alternating sand and silt laminae resulting in non-uniform distribution of matrix (Fig.5a). The sand laminae have better porosity and pore connectivity than the silt laminae. The silt laminae have higher matrix density with lower porosity due to iron oxides, silt size quartz and clay filling most of the pores in the silt laminae. They have an average porosity of 19.8% and permeability of 113.2mD (Table 1). The porosity type is mainly intergranular with fair pore connectivity.

#### **4.1.5. Massive fine grained sandstone**

The massive fine grained sandstones can be divided into two subfacies; the moderately sorted sandstones and poorly sorted sandstones. The division of this facies into two subfacies is as a result of the significant difference in their porosity and permeability.

The moderately sorted fine grained sandstones are composed mainly of quartz and feldspars with minor amount of iron oxides and clays (kaolinite) (Figs.6a-6f). The kaolinite occur mainly as pore-filling clays filling the intergranular pores between the grains (Figs.6c-6d). The pore connectivity is fair to good with relatively uniform distribution of matrix. They have an average porosity of 24.7% and permeability of 402.1mD. They have subangular and moderately sorted grains with predominantly fine grains ranging in sizes between 65-165microns. They are massive structured in both micro and meso scale.

The poorly sorted fine grained sandstone have subangular and poorly sorted grains with predominantly fine grains ranging in sizes between 82-276microns (Figs.7a and 7b). Significant amount of pore-filling clays (kaolinite) occur in intergranular pores in these samples (Figs.7c-7d). They are composed mainly of quartz and feldspars with minor amount of iron oxides (Figs.7a, 7e and 7f). Pore connectivity is fair with relatively uniform distribution of matrix. The poorly sorted fine grained sandstones have an average porosity of 19.9% and permeability of 100.4mD (Table 1).

## **4.2. Facies and Porosity-Permeability Relationships**

A comparison of the porosity and permeability between the facies indicate that coarse grained sandstones have the highest porosity and permeability as opposed to the very low porosity and permeability recorded in the very fine grained sandstones. Porosity and permeability for the coarse grained sandstones range from 21.5%-30.42% with a mean of 24.97% and 1250.2mD-2913.56mD with a mean of 1910.6mD respectively. The relatively higher porosity and permeability in the coarse grained sandstone can be attributed to the lack of significant cement between the grains, abundant visible macro intergranular pores and very good pore connectivity within the samples. Porosity and permeability for the very fine grained sandstones range from 0.17%-13.5% with a mean of 5.66% and 0.1mD-5.39mD with a mean of 1.4mD respectively. The relatively lower porosity and permeability in this facies is due to the absent of significant pore space between the grains. Most of the pores in the sample have been filled by matrix, cement and pore-filling clays (kaolinite) resulting in highly consolidated samples.

Significant reduced porosity and permeability is recorded in the bioturbated sandstones compared to the non-bioturbated sandstones. Porosity and permeability in the bioturbated sandstones range from 10.6%-19.7% with a mean of 16.48% and 5.95mD-47.9mD with a mean of 23.28mD respectively. The poorly sorted massive sandstones have porosity and permeability range from 16.7%-23.4% with a mean of 19.85% and 52.27mD-172mD with a mean of 100.36mD respectively. Such reduction in porosity and permeability in the bioturbated sandstones can be attributed to sediment mixing activity by burrowing organisms [30-32]. Such burrowing activity leads to selective concentration of clay, iron oxides, pyrite and heavy minerals within burrows as compared to host sandstone matrix. The EDX mapping of the

burrow fill show the presence of pyrite, kaolinite and heavy minerals such as titanium and manganese within the burrows.

The influence of sorting on porosity and permeability in these sandstone facies of the Baram delta is observed in the variation of these petrophysical properties between the poorly sorted fine grained massive sandstones and moderately sorted fine grained massive sandstones. Porosity and permeability in the moderately sorted sandstone are relatively much higher ranging from 17.7%-32.1% and 223.34mD-672.84mD respectively compared to 16.7%-23.4% and 52.27mD respectively in the poorly sorted sandstones. In addition to sorting, the higher amount of pore-filling clays in the pores of the poorly sorted sandstones also significantly reduces porosity.

### 4.3. Displacement Pressure, Pore Size Distribution and Irreducible Water Saturation

The very fine sandstones have the highest displacement pressure of 59.94Psi (Table 2). This can be correlated directly with the small pore throat sizes/ micro pores in the very fine grained sandstones. Smaller pores require higher displacement pressures to move hydrocarbons into the sample. Average pore throat diameter in the very fine grained samples is 0.268 microns putting most of the pores in the micro pores range (Table 2). The moderately sorted fine grained sandstones and coarse grained sandstones have the lowest displacement pressures of 4.076 and 8.702 corresponding to average pore diameters of 8.273 and 5.129 respectively (Table 2). These pore sizes are within the macro pores range. Bigger pores sizes therefore correlate to lower displacement pressure and vice versa as observed in these facies.

Table 2. Displacement pressure, average pore diameter, pore type, maximum pore diameter, median pore diameter and irreducible water saturation for the different facies

Facies	Displacement Pressure (Psi)	Average Pore Diameter (microns)	Pore type	Max. Pore Diameter (microns)	Median Pore Diameter (microns)	Irreducible water saturation (%)
Very fine sandstone	59.944	0.268	Micro	59.57089	0.25397	87.3
Coarse sandstones	8.702	5.129	Macro	100.87828	16.87752	5.2
Moderately sorted sandstone	4.076	8.273	Macro	111.00418	34.04244	6.7
Poorly sorted sandstone	11.603	0.557	Meso	100.32779	8.78503	3
Bioturbated sandstones	10.153	1.437	Meso	113.13887	10.95177	8.1
Laminated sandstones	14.504	1.044	Meso	110.33798	7.36754	6.6

Characteristic of the variable textural variations in most bioturbated samples, two distinct pore size distribution trends (bimodal) (Figure 8f) are observed in these samples reflecting the two main different textural domains arising from the presence of ichnofabrics and host sandstones. The parallel laminated sandstones also show bimodal distribution of pores corresponding to the two types of lamination; sand-dominated and silt-dominated laminations in these samples with the sand-dominated lamination having the bigger pore sizes (Figure 8c). The fine-grained poorly sorted sandstones show a wider range of pore sizes which is consistent with their poorly sorted nature.

A comparative analysis of the mercury capillary pressure distribution curves show two distinct group of curves between the six sandstone facies (Figs.8a-8e). The very fine grained sandstones have a very distinct curve (Fig.8d) compared to the other facies. The very fine grained sandstones have a steep curve indicating a non-uniform distribution of pores in the sample that requires correspondingly high displacement pressure to inject mercury into the pores. The other five facies have capillary pressure curves with long and flat plateau. The long and flat plateau capillary curve indicates uniform distribution and relatively well sorted pore throat sizes. This means that in facies with these curves, once the displacement pressure

which is relatively low is achieved, only small incremental pressures are required to inject mercury into the pores.

The irreducible water saturation is equivalent to the percentage of water adsorbed onto mineral surfaces and in pores that cannot be removed at the maximum pressure. The very fine grained sandstone have the highest irreducible water saturation of 87.3%. The rest of the pore volume in this sample (12.7%) is saturated with mercury at maximum pressure. This can be attributed to the predominantly small pores (micro pores). At reservoir conditions, this facies traps high amount of water within the pores and should have low hydrocarbon recovery. The poorly sorted sandstones and coarse grained sandstones have the lowest irreducible water saturation of 3% (97% of mercury saturation) and 5.2% (94.8% of mercury saturation) respectively. At reservoir conditions, hydrocarbons can therefore easily migrate into these reservoir types at low displacement pressure.

## 5. Conclusion

This study of some selected petrophysical properties of reservoir rocks of the West Baram Delta has allowed for a comprehensive analysis of the variations in petrophysical properties between the major reservoir facies. Six sandstone lithofacies were identified in all the wells: coarse sandstone, very fine sandstone, massive fine sandstone (poorly sorted and moderately sorted), bioturbated sandstone and laminated sandstone. The alternating sequences of mudstones, siltstones and sandstones in all the wells are consistent with the prograding nature of the Baram Delta. Petrographic analysis indicates that grain size, sorting, bioturbation and subsequent diagenesis are suggested as major controls on petrophysical variations of reservoir rocks in the Baram Delta.

Among the sandstone facies, the coarse grained sandstones are the best in terms of reservoir rock quality. They have the highest porosity and permeability values, and very low displacement pressure and irreducible water saturation. This is mainly due to their relatively uniform pore size distribution, large intergranular pores, lack of cement between grains and excellent pore connectivity. The very fine grained sandstones are the poorest in terms of reservoir rock quality. They have extremely low porosity and permeability, and very high displacement pressure and irreducible water saturation. This is due to their highly consolidated nature resulting in very high amount of cement filling all the pores between grains resulting in very poor pore connectivity and non-uniform distribution of pores.

Results of the study show that the six main facies identified are characterized by distinctive MICP type curves, pore size and pore type distribution. The tight very fine grained sandstones are dominated by nanopores and micropores. The MICP curves for this facies are very steep indicating a non-uniform distribution of pores in the sample that require correspondingly high displacement pressure to inject mercury into the pores. Therefore, at reservoir conditions these massive very fine grained sandstones trap high amount of water within the pores due to high capillary pressure and should have low hydrocarbon recovery and high irreducible water saturation. The curves for massive coarse grained sandstones and moderately sorted fine grained sandstones show relatively less steep curves indicating a more uniform distribution of well sorted pores. The massive coarse grained sandstones have the biggest pore sizes that fall within the upper macro range. The bioturbated sandstones with two textural domains (burrowed zones and non-burrowed zones) are characterized by bimodal pore size distribution representative of the two zones. The parallel laminated sandstones composed of alternating sand and silt-dominated lamination are also characterized by bimodal pore size distribution. The less porous silt-dominated laminations consist of micropores to mesopores whereas the more porous sand-dominated laminations are dominated by lower to upper macro pores.

**Figures 2-8**

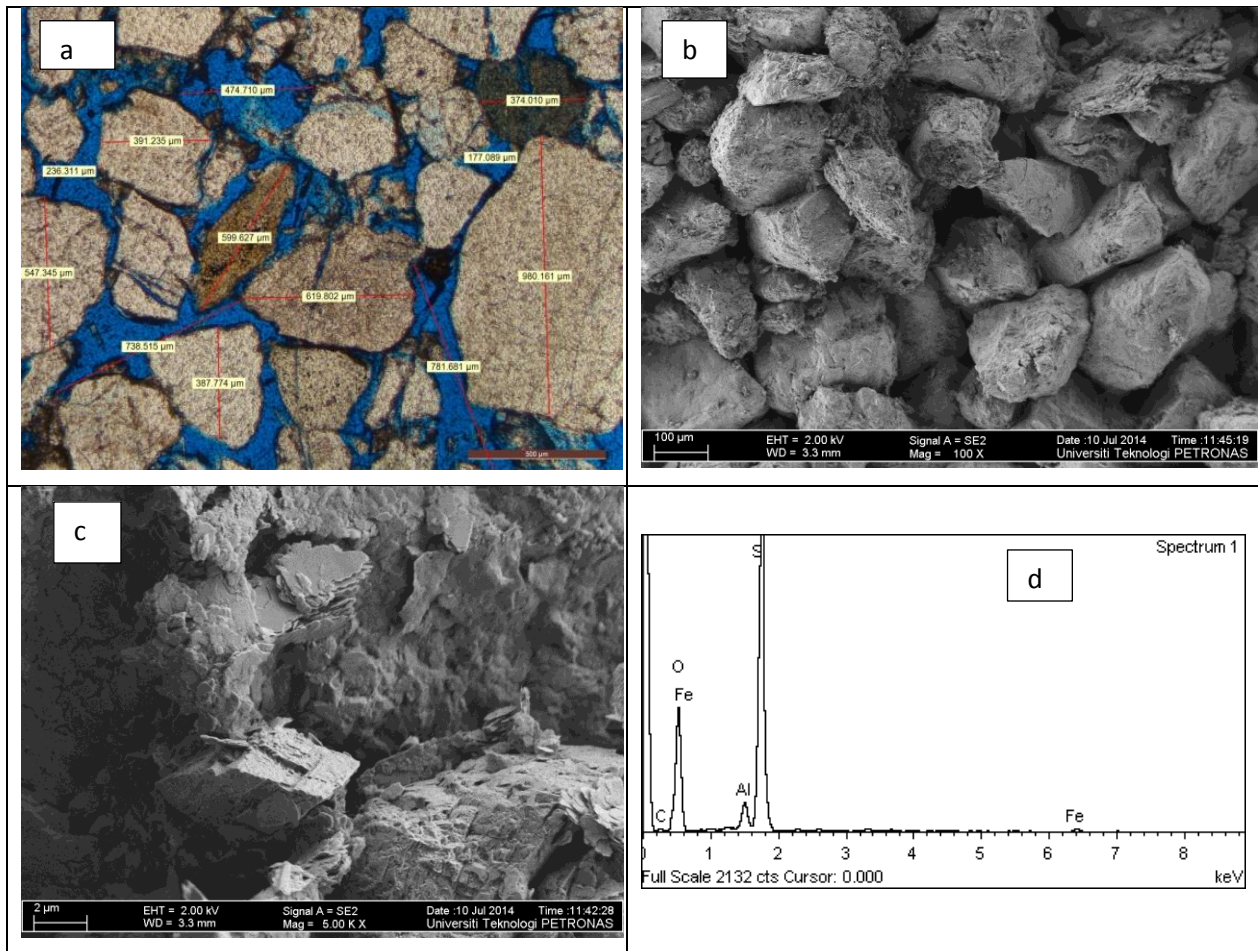


Fig. 2. (a) Thin section photomicrograph of coarse grained sandstone showing predominantly coarse grains, very good intergranular porosity dominated by macro pores, good pore connectivity, quartz as the dominant framework grain, mica and in-situ alteration of glauconite; SEM photomicrographs of coarse grained sandstone showing (b) moderate sorting of sand grains and (c) minor amount of clays on grain surfaces and in pores; (d) EDX showing elemental composition of coarse grained sandstone

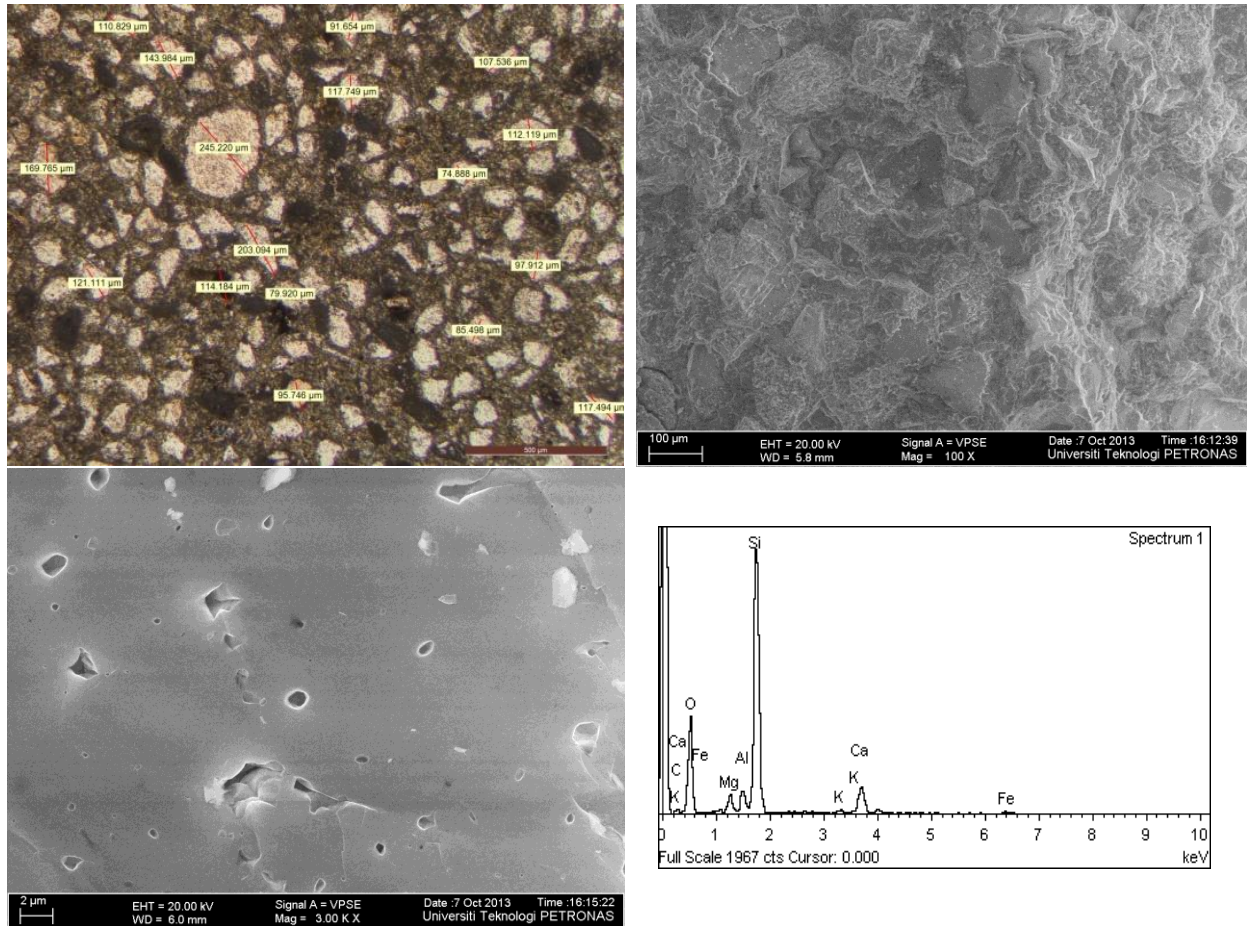


Fig. 3. (a) Thin section photomicrograph of very fine grained sandstone showing predominantly very fine grains, lack of intergranular porosity, high matrix density and poor sorting; SEM photomicrographs of very fine grained sandstone showing (b) very high consolidation of grains and lack of intergranular pores and (c) minor amount of micro pores; (d) EDX showing elemental composition of very fine grained sandstone

A	B
C	D

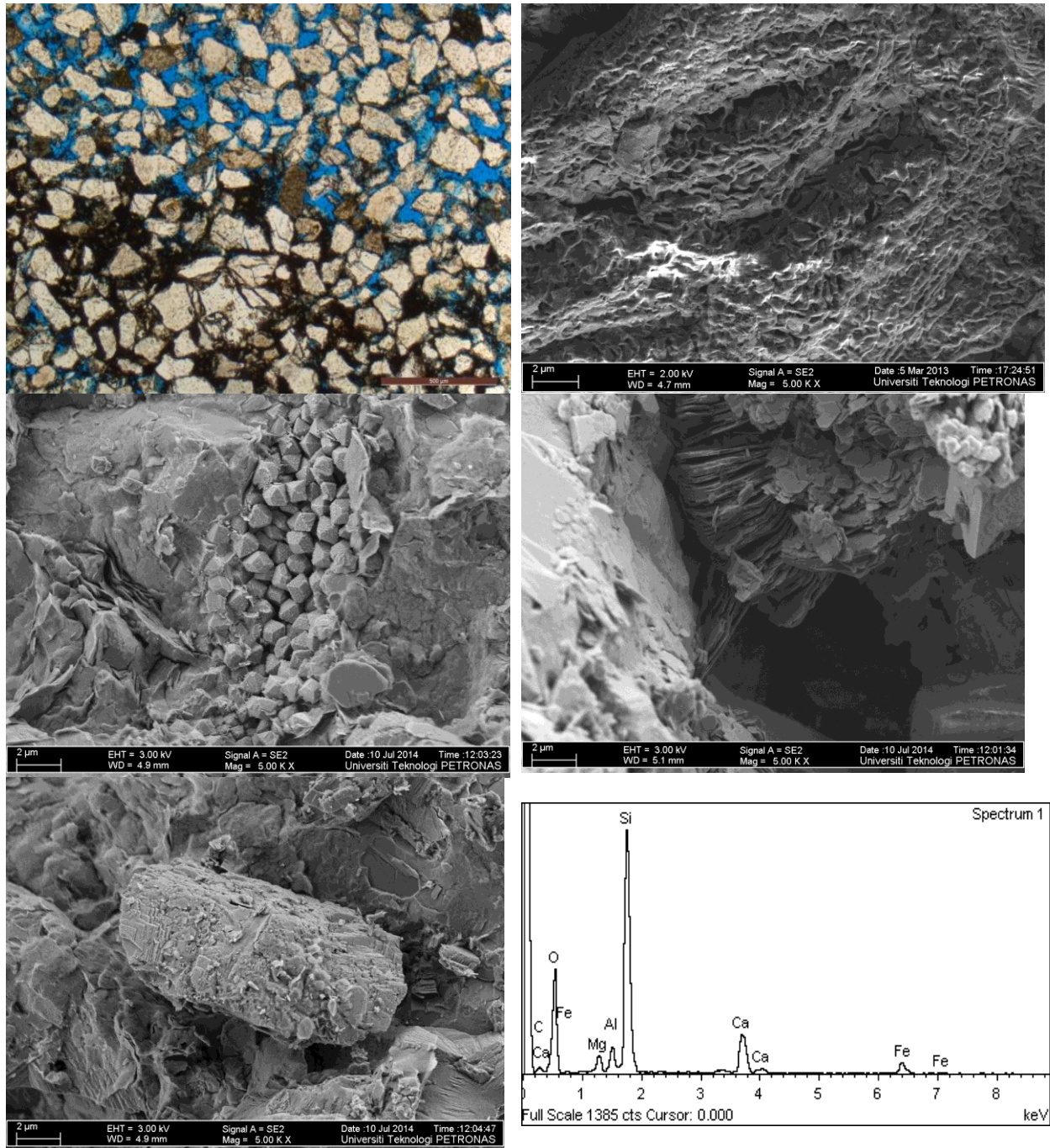


Fig. 4. (a) Thin section photomicrograph of bioturbated sandstone showing predominantly fine grain quartz as dominant framework, non-uniform distribution of matrix between burrow and host sandstone, variation in intergranular porosity and pore connectivity between burrow and host sandstone and poor sorting; SEM photomicrographs of bioturbated sandstone showing (b) burrow mottled texture by burrowing organisms (c) pyrite crystals in burrows (d) pore-filling kaolinite and (e) feldspars; EDX showing (f) elemental composition of bioturbated sandstone

A	B
C	D
E	F

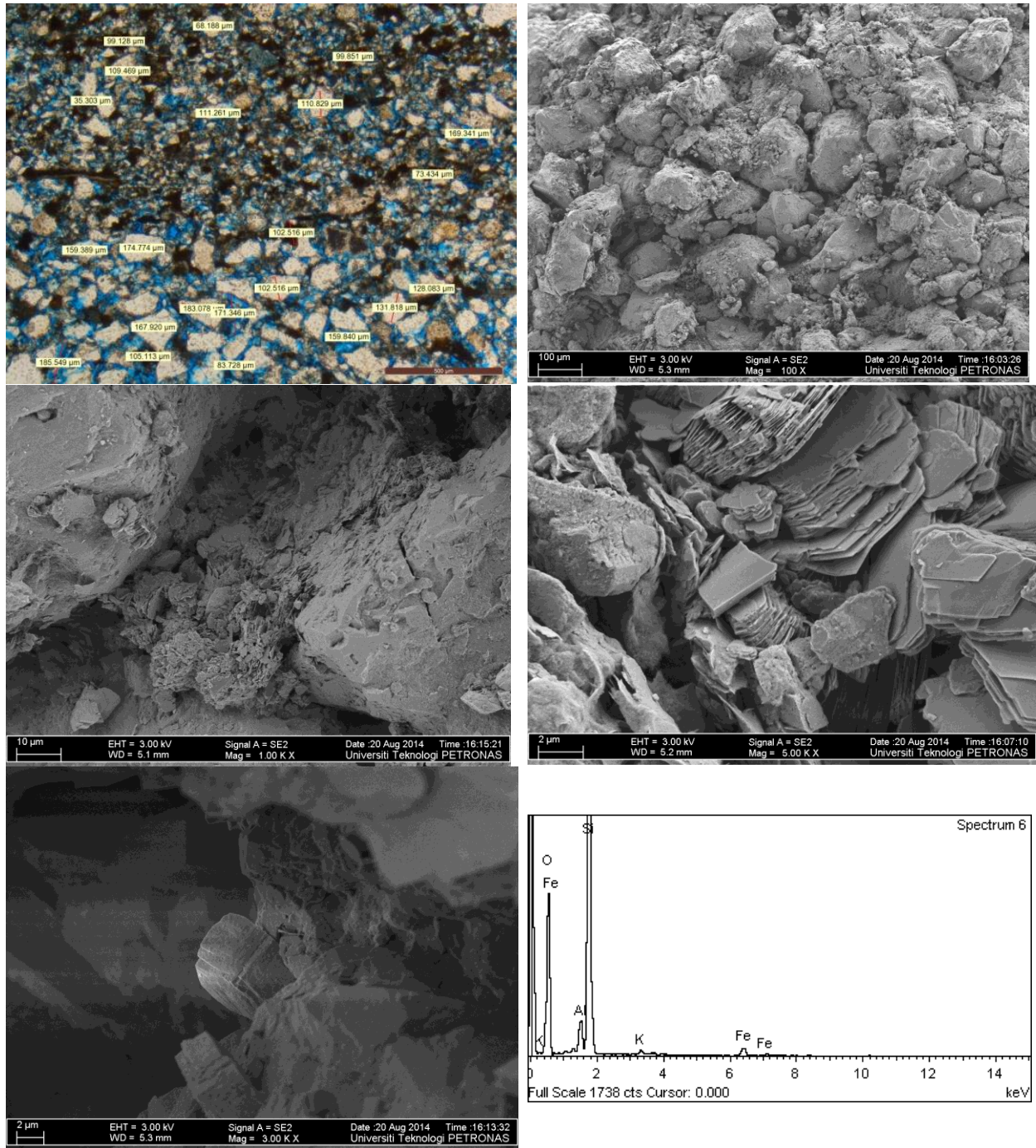


Fig. 5. (a) Thin section photomicrograph of laminated sandstone showing alternating sand and silt dominated lamina, non-uniform distribution of matrix between sand lamina and silt lamina, variation in intergranular porosity and pore connectivity between sand lamina and silt lamina and poor sorting; SEM photomicrographs of laminated sandstone showing (b) poorly sorted grains (c) pore-filling clays (d) pore-filling kaolinite and (e) feldpars; EDX showing (f) elemental composition of laminated sandstone

A	B
C	D
E	F

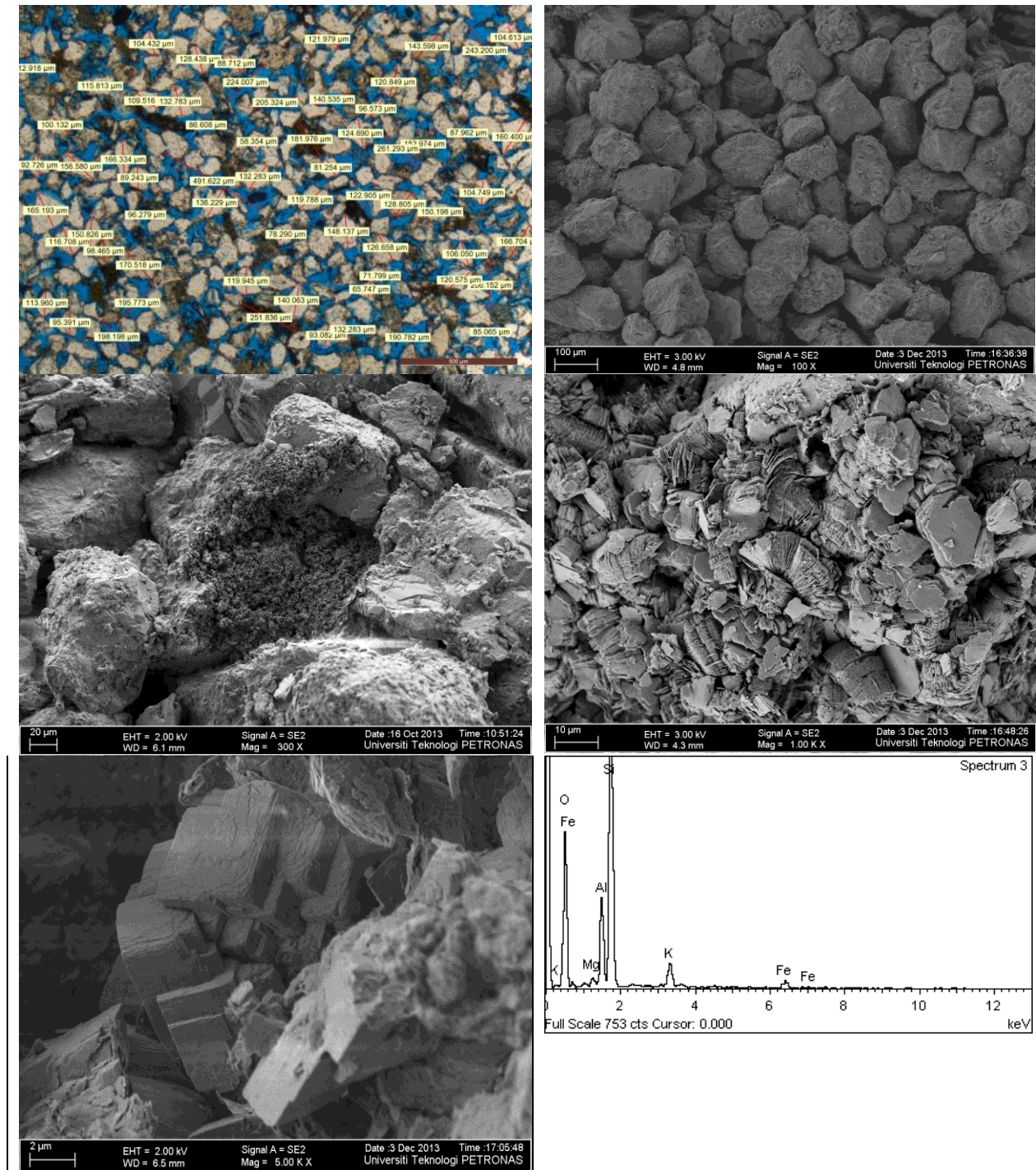


Fig. 6. (a) Thin section photomicrograph of moderately sorted fine sandstone showing predominantly fine grain quartz as dominant framework, relatively good intergranular porosity and pore connectivity; SEM photomicrographs of moderately sorted fine sandstones showing (a) moderate sorting (b) pore-filling clay (c) pore-filling kaolinite (d) pore-filling kaolinite and (e) feldspars (f) EDX showing elemental composition of moderately sorted fine sandstone

A	B
C	D
E	F

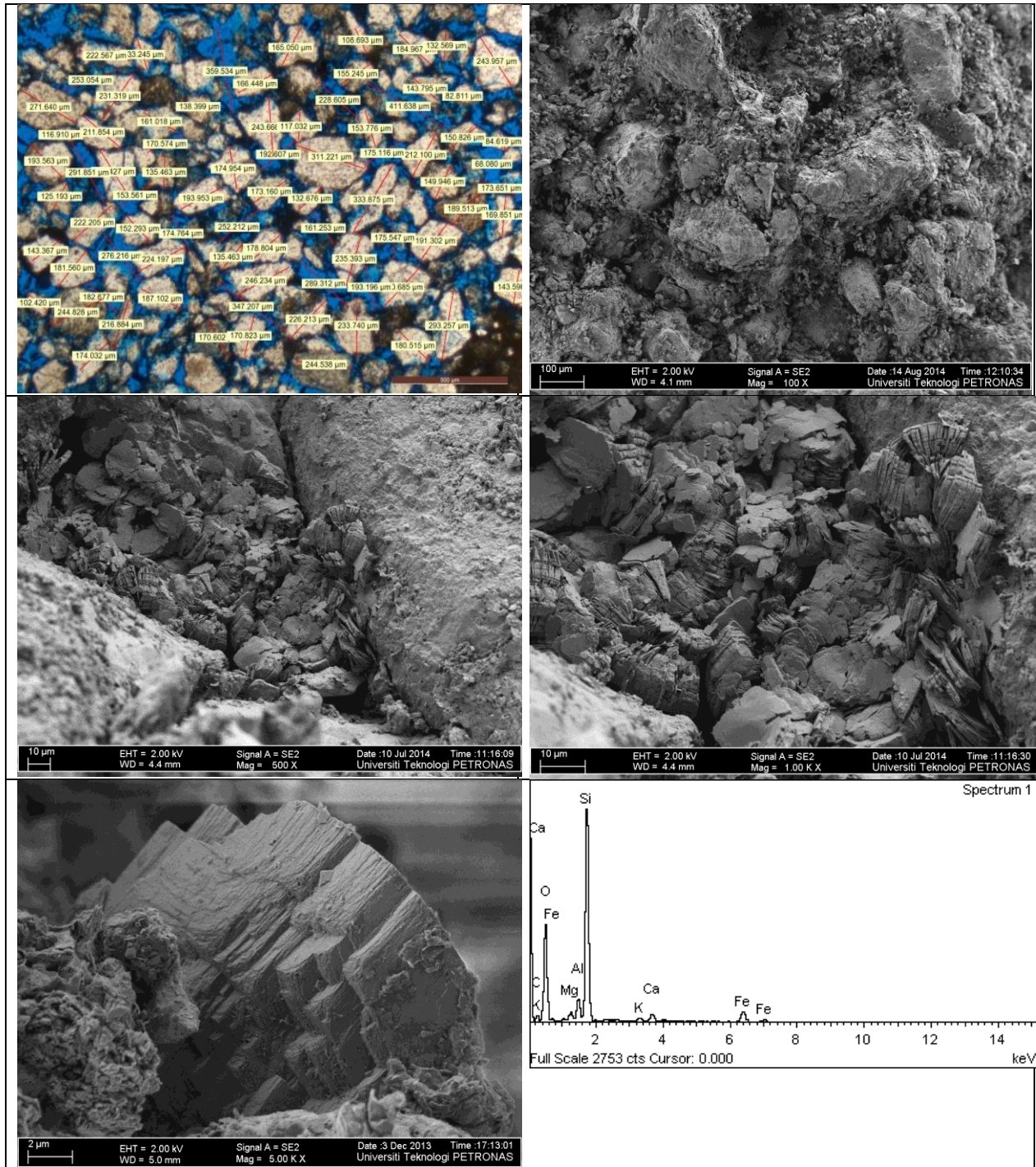


Fig. 7. (a) Thin section photomicrograph of poorly sorted massive sandstone showing predominantly fine quartz as dominant framework, good intergranular porosity and pore connectivity; SEM photomicrographs of poorly sorted massive sandstone showing (b) poor sorting (c) pore-filling clays (d) pore-filling kaolinite and (e) feldspars; (f) EDX showing elemental composition of poorly sorted massive sandstone

A	B
C	D
E	F

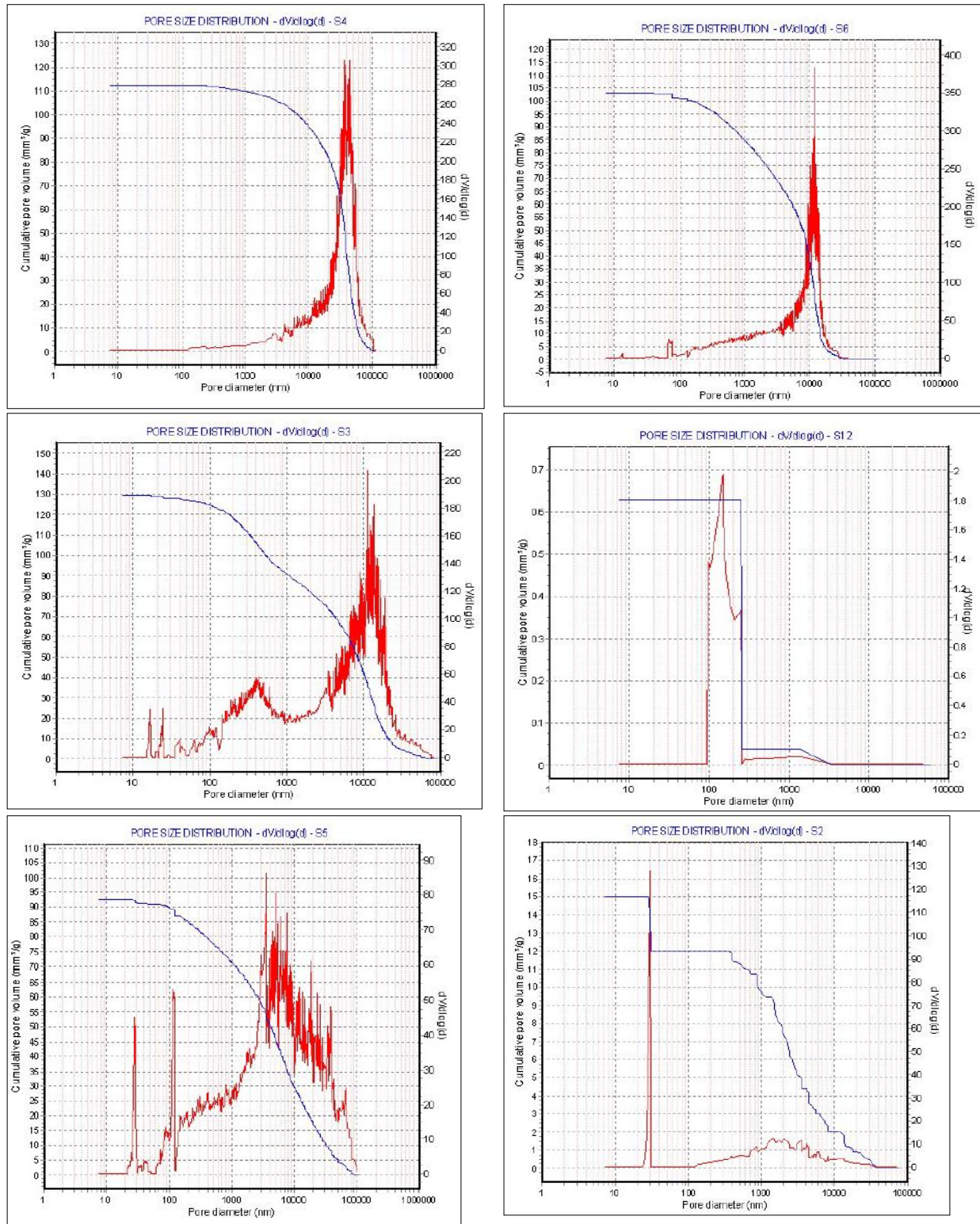


Fig. 8. Pore size distribution and capillary pressure curves for (a) massive coarse grained sandstones (b) massive fine grained sandstone-moderately sorted (c) parallel laminated sandstone (d) massive very fine grained sandstone (e) massive fine grained sandstone-poorly sorted and (f) bioturbated sandstone

<b>A</b>	<b>B</b>
<b>C</b>	<b>D</b>
<b>E</b>	<b>F</b>

## References

- [1] Selly RC. 1996. Ancient sedimentary environments and their sub-surface diagnosis, Chapman and Hall, 300pp.
- [2] Alpay O A. 1972. A practical approach to defining reservoir heterogeneity: Journal of Petroleum Technology, v. 1972, p. 841–848.
- [3] Evans RC. 1987. An investigation into the influence of common sedimentary structures and diagenesis on permeability heterogeneity and anisotropy in selected sands and sandstones. Society of Petroleum Engineers Paper 17130.
- [4] Moraes MA and Surdam RC. 1993. Diagenetic heterogeneity and reservoir quality; fluvial, deltaic, and turbiditic sandstone reservoirs, Potiguar and Reconcavo rift basins, Brazil. AAPG Bulletin, July 1993, v. 77, pp. 1142-1158.
- [5] Morad S, Al-Ramadan K, Ketzer JM, and De Ros LF. 2010, The impact of diagenesis on the heterogeneity of sandstone reservoirs: A review of the role of depositional facies and sequence stratigraphy. American Association of Petroleum Geologists (AAPG) Bulletin, 94, pp.1267 – 1309.
- [6] Jensen J and Currie I. 1990. A new method for estimating the Dykstra-Parsons coefficient to characterize reservoir heterogeneity. SPE Reservoir Engineering, p.369-374.
- [7] Roller C, Driskil, B and Manrique J. 2009. Use of the Allan variance for characterizing reservoir heterogeneity. Society of Petrophysicists and Well Log Analysts (SPWLA) 50th Annual Logging Symposium, Woodlands, Texas.
- [8] Ho KF. 1978. Stratigraphic framework for oil exploration in Sarawak. Bulletin of the Geological Society of Malaysia, 10, pp.1-13.
- [9] Madon M, Cheng LyK and Wong R. 2013. The structure and stratigraphy of deepwater Sarawak, Malaysia: Implications for tectonic evolution. Journal of Asian Earth Sciences, 76, pp.312-333.
- [10] Tan DNK, Rahman AHB, Anuar A, Bait B and Tho CK. 1999. West Baram Delta. In: Meng, L.K. (Editor) The Petroleum Geology and Resources of Malaysia. PETRONAS. pp. 291-341.
- [11] Hiscott R.2001. Depositional sequences controlled by high rates of sediments supply, sea level variations and growth faulting: the Quaternary Baram delta of northwestern Borneo. Journal of Marine Geology, v.175, pp.67-102.
- [12] Lambiase J, Rahim,AA and Peng CY. 2002. Facies distribution and sedimentary processes on the modern Baram Delta: implications for the reservoir sandstones of NW Borneo. Marine and Petroleum Geology, Elsevier, p.69-72.
- [13] Hutchinson CS. 2005, Geology of North West Borneo: Sarawak, Brunei and Sabah. 1<sup>st</sup> ed., Elsevier, New York, USA, 421p.
- [14] Madon M. 1999. Geological Setting of Sarawak. In: Meng, L. K. (Eds.), The Petroleum Geology and Resources of Malaysia. Petroliaam Nasional Berhad (PETRONAS), Kuala Lumpur, 275-290.
- [15] Amir Hassan MH, Johnson HD, Allison PA and Abdullah WH. 2013. Sedimentology and stratigraphy development of the Upper Nyalau Formation (Early Miocene), Sarawak, Malaysia: A mixed wave-and tide-influenced coastal system, 76, pp.301-311.
- [16] Abd. Rahman AH, Menier D, Mansor YM. 2014. Sequence Stratigraphic Modeling and Reservoir Architecture of the Shallow Marine Successions of Baram Field, West Baram Delta, Offshore Sarawak, East Malaysia. Marine and Petroleum Geology, 58, 687-703.
- [17] Molnar P and Tapponnier, 1975. Cenozoic tectonics of Asia: effects of a continental collision. Science, New Series, 189(4201), pp.419-426.

- [18] Hall R 2002. Cenozoic geological and plate tectonics evolution of SE Asia and the SW Pacific: computer-based reconstructions, model and animations. *Journal of Asian Earth Sciences*, v.20, pp.353-431.
- [19] Ryan WBF, Carbotte SM, Coplan JO, O'Hara S, Melkonian A, Arko R, Zemsky R. 2009. Global Multi-Resolution Topography Synthesis. *Geochemistry Geophysics Geosystems*, 10, 1-3.
- [20] Cullen A. 2014. Nature and significance of the West Baram and Tinjar Lines, NW Borneo. *Marine and Petroleum Geology*, 51, p.197-209.
- [21] Surdiman SB, Samsudin YB and Darman NH. 2007. Planning for regional EOR pilot for Baram Delta, offshore Sarawak, Malaysia: Case study, lessons learnt and way forward. SPE Asia Pacific Oil and Gas conference and Exhibition, Jakarta, Indonesia.
- [22] Bakar MA, Chong YY, Nasir E, Din A, Fui CC, Adamson G, Agarwal B and Valdez R. 2011, EOR evaluation for Baram Delta operations fields, Malaysia. Society for Petroleum Engineering (SPE) Enhanced Oil Recovery Conference, 19-21 July 2011, Kuala Lumpur, Malaysia.
- [23] Rijks EJH. 1981. Baram Delta geology and hydrocarbon occurrence (Sarawak). *Geol. Soc. Malays. Bull.* 14, 1-8.
- [24] Johnson HD, Kudd T and Dundang A. 1989. Sedimentology and reservoir geology of the Betty field, Baram Delta Province, offshore Sarawak, NW Borneo. *Bulletin of Geologic Society of Malaysia*, 25, p.119-161.
- [25] Tucker ME. 1988. *Techniques in Sedimentology*. Wiley. p.394.
- [26] Jerram DA. 2001, Visual comparators for degree of grain size sorting in two and three-dimensions. *Computers and Geoscience*, 27, 485-492.
- [27] Raith MM, Raase P and Reinhardt J. 2011. Guide to thin section microscopy. p.107.
- [28] Trewin N. 1988. Use of scanning electron microscope in sedimentology. In: M.E. Tucker (Ed), *Techniques in sedimentology*, pp.229-273.
- [29] Welton JE. 1984. SEM petrology atlas, American Association of Petroleum Geologists, p.240.
- [30] Tonkin NS, McIlroy D, Meyer R, Moore-Turpin A. 2010, Bioturbation influence on reservoir quality: a case study from the Cretaceous Ben Nevis Formation, Jeanne d'Arc Basin, offshore Newfoundland, Canada. *American Association of Petroleum Geologist Bulletin (AAPG)*, 94, 1059-1078.
- [31] Ben-Awuah J, Padmanabhan E. 2014. Impact of Bioturbation on Reservoir Quality: A Case Study of Biogenically Reduced Permeabilities of Reservoir Sandstones in the Baram Delta, Sarawak, Malaysia. *Journal of Applied Sciences*, 14, 3312-3317.
- [32] Ben-Awuah J, Padmanabhan E. 2015. Effect of Bioturbation on Reservoir Rock Quality of Sandstones: A Case Study from the Baram Delta, offshore Sarawak, Malaysia. *Petroleum Exploration and Development*, 42, 1-9.

---

\* Corresponding author email address: [jbenawuah@gmail.com/](mailto:jbenawuah@gmail.com)  
[benawuah@ucsiuniversity.edu.my](mailto:benawuah@ucsiuniversity.edu.my)